Constraining the dark energy models with $H(z)$ data: An approach independent of H_0

Fotios K. Anagnostopoulos[1,*] and Spyros Basilakos[2,†]

[1]National and Kapodistrian University of Athens, Physics Department, Panepistimioupoli Zografou, 15772 Athens, Greece

[2]Academy of Athens, Research Center for Astronomy and Applied Mathematics, Soranou Efesiou 4, 11527 Athens, Greece

(Received 11 September 2017; published 2 March 2018)

We study the performance of the latest $H(z)$ data in constraining the cosmological parameters of different cosmological models, including that of Chevalier-Polarski-Linder w_0w_1 parametrization. First, we introduce a statistical procedure in which the chi-square estimator is not affected by the value of the Hubble constant. As a result, we find that the $H(z)$ data do not rule out the possibility of either nonflat models or dynamical dark energy cosmological models. However, we verify that the time varying equation-of-state parameter $w(z)$ is not constrained by the current expansion data. Combining the $H(z)$ and the Type Ia supernova data, we find that the $H(z)$/SNIa overall statistical analysis provides a substantial improvement of the cosmological constraints with respect to those of the $H(z)$ analysis. Moreover, the $w_0 - w_1$ parameter space provided by the $H(z)$/SNIa joint analysis is in very good agreement with that of Planck 2015, which confirms that the present analysis with the $H(z)$ and supernova type Ia (SNIa) probes correctly reveals the expansion of the Universe as found by the team of Planck. Finally, we generate sets of Monte Carlo realizations in order to quantify the ability of the $H(z)$ data to provide strong constraints on the dark energy model parameters. The Monte Carlo approach shows significant improvement of the constraints, when increasing the sample to 100 $H(z)$ measurements. Such a goal can be achieved in the future, especially in the light of the next generation of surveys.

DOI: 10.1103/PhysRevD.97.063503

I. INTRODUCTION

The general picture of the cosmos, as it is established by the analysis of the recent cosmological data (see Ref. [1] and references therein), is described with a cosmological scenario that consists ∼30% of matter (baryonic and dark) while the rest corresponds to the so-called dark energy (DE). This mysterious component of the cosmic fluid plays an eminent role in cosmological studies because it is responsible for the accelerated expansion of the Universe. Also, current observations seem to favor an isotropic, homogeneous, and spatially flat universe.

During the last decades, different classes of theoretical models have been introduced in order to explain the accelerating Universe,[1] giving rise to a scholastic debate about what is the exact description and the key points of each scheme. One of the fundamental questions of modern cosmology that subsequently emerges is what is the model that best describes the accelerated expansion of the Universe [3]. A prominent path in order to distinguish the various cosmological models is to probe the cosmic history [4] of the Universe, using either the luminosity distance of standard candles or the angular diameter distance of standard rulers.

In order to map the cosmic expansion history, it is common to use a combination of various cosmological probes, namely standard candles (SNIa [5,6], gamma ray bursts, [7], HII galaxies [8,9]), standard rulers (clusters, baryon acoustic oscillations (BAOs), [10,11]), the cosmic microwave background (CMB) angular power spectrum [1] and recently, data from gravitational wave measurements, the so-called standard sirens [12]. Alternatively, dynamical probes of the expansion history based on measures of the growth rate of matter perturbations (for recent studies, see Ref. [13] and references therein) are also used toward tracing the cosmic expansion, and they are confined to relatively low redshifts similar to those of Type Ia supernova data $z \simeq 1.4$. The aforementioned observations probe the integral of the Hubble parameter $H(z)$; hence, they give us indirect information for the cosmic expansion. Also, it is worth noting that in some cases the data suffer from the so-called circularity problem, the fact that one needs to impose a fiducial cosmology in order to be able to define the data (see for example Refs. [14,15]).

*fotis-anagnostopoulos@hotmail.com
†svasil@academyofathens.gr

[1]For a review, see Ref. [2].

Among the large body of cosmological data, the only data set that provides a direct measurement of the cosmic expansion is the $H(z)$ sample, and indeed a plethora of papers have been published (e.g. Refs. [16–31]) which determine the dynamical characteristics of various DE cosmological models, including those of modified gravity. Today, the most recent $H(z)$ data trace the cosmic expansion rate up to redshifts of order $z \simeq 2.4$, while there are proposed methods [32] which potentially could expand the $H(z)$ measurements to $z \leq 5$. As expected, using the $H(z)$ data in constraining the cosmological models via the standard likelihood analysis, one has to deal with the Hubble constant, namely H_0. However, the best choice of the value of H_0 is rather uncertain. Indeed, several studies on the determination of the Hubble constant have indicated a $\sim 3.1\sigma$ tension between the value obtained by the Planck team (see Ref. [1]), namely $H_0 = 67.8 \pm 0.9$ Km/s/Mpc, and the results provided by the SNIa project (Riess *et al.* [33]) of $H_0 = 73.24 \pm 1.74$ Km/s/Mpc. In order to alleviate this problem, we propose in the current work a statistical method which is not affected by the value of H_0.

The structure of the article is as follows. In Sec. II, we present the $H(z)$ data used and the related statistical analysis. At the beginning of Sec. III, we describe the main properties of the most basic DE models, and then we focus on the cosmological constrains. In Sec. IV, we discuss the Monte Carlo simulations used toward planning future $H(z)$ measurements in order to place better constraints on the DE model parameters. Finally, in Sec. V, we provide a detailed discussion of our results, and we summarize our conclusions in Sec. VI.

II. STATISTICAL ANALYSIS WITH $H(z)$ DATA

In this section, we discuss the details of the statistical analysis and on the observational sample that we utilize in order to place constraints on the cosmological parameters. In particular, we use the cosmic expansion data as collected by Farooq *et al.* [28] (see Table I and the corresponding references) for which the Hubble parameter is available as a function of redshift. Notice, that the $H(z)$ sample contains 38 entries in the following redshift range: $0.07 \leq z \leq 2.36$. In Fig. 1, we present the normalized redshift distribution of the $H(z)$ data and the corresponding distribution of the relative uncertainty $\sigma(\%) = \sigma_{H(z_i)}/H(z_i)$. Also, we find no significant correlation between σ and redshift in that range.

First, let us assume that we have a dark energy model that includes n-free parameters, provided by the statistical vector $\phi^\mu = (\phi^0, \phi^1, \ldots \phi^n)$. In order to put constraints on ϕ^μ, we need to implement a standard χ^2-minimization procedure, which in our case is written as

$$\chi^2(\phi^\mu) = \sum_{i=1}^{N} \left[\frac{H_D(z_i) - H_M(z_i, \phi^\mu)}{\sigma_i} \right]^2, \qquad (1)$$

TABLE I. The observational data set that was used in this paper. The data set, compiled by Farooq *et al.* [28] consists of $N = 38$ observations.

z	$H(z)$ (Km/s/Mpc)	σ_H (Km/s/Mpc)	Method/Reference
0.070	69.0	19.6	[34]
0.090	69.0	12.0	[35]
0.120	68.6	26.2	[34]
0.170	83.0	8.0	[35]
0.179	75.0	4.0	[36]
0.199	75.0	5.0	[36]
0.200	72.9	29.6	[34]
0.270	77.0	14.0	[35]
0.280	88.8	36.6	[34]
0.352	83.0	14.0	[36]
0.380	81.5	1.9	[11]
0.3802	83.0	13.5	[37]
0.400	95.0	17.0	[35]
0.4004	77.0	10.2	[37]
0.4247	87.1	11.2	[37]
0.440	82.6	7.8	[38]
0.4497	92.8	12.9	[37]
0.4783	80.9	9.0	[37]
0.480	97.0	62.0	[39]
0.510	90.4	1.9	[11]
0.593	104.0	13.0	[36]
0.600	87.9	6.1	[38]
0.610	97.3	2.1	[11]
0.680	92.0	8.0	[36]
0.730	97.3	70.0	[38]
0.781	105.0	12.0	[36]
0.875	125.0	17.0	[36]
0.880	90.0	40.0	[39]
0.900	117.0	23.0	[35]
1.037	154.0	20.0	[36]
1.300	168.0	17.0	[35]
1.363	160.0	33.6	[40]
1.430	177.0	18.0	[35]
1.530	140.0	14.0	[35]
1.750	202.0	40.0	[35]
1.965	186.5	50.4	[40]
2.340	222.0	7.0	[41]
2.360	226.0	8.0	[42]

where $H_D(z_i)$ and σ_i are the observational data and the corresponding uncertainties at the observed redshift, z_i. The capital letters M and D stand for model and data respectively. In this case, the theoretical Hubble parameter is written as

$$H_M(z, \phi^\mu) = H_0 E(z, \phi^{\mu+1}), \qquad (2)$$

where H_0 is the current value of Hubble parameter, namely the Hubble constant; $E(z)$ is the normalized Hubble function; and the vector ϕ^μ contains the cosmological parameters. In this framework, we observe that the statistical vector becomes $\phi^\mu = (H_0, \phi^{\mu+1})$, where the

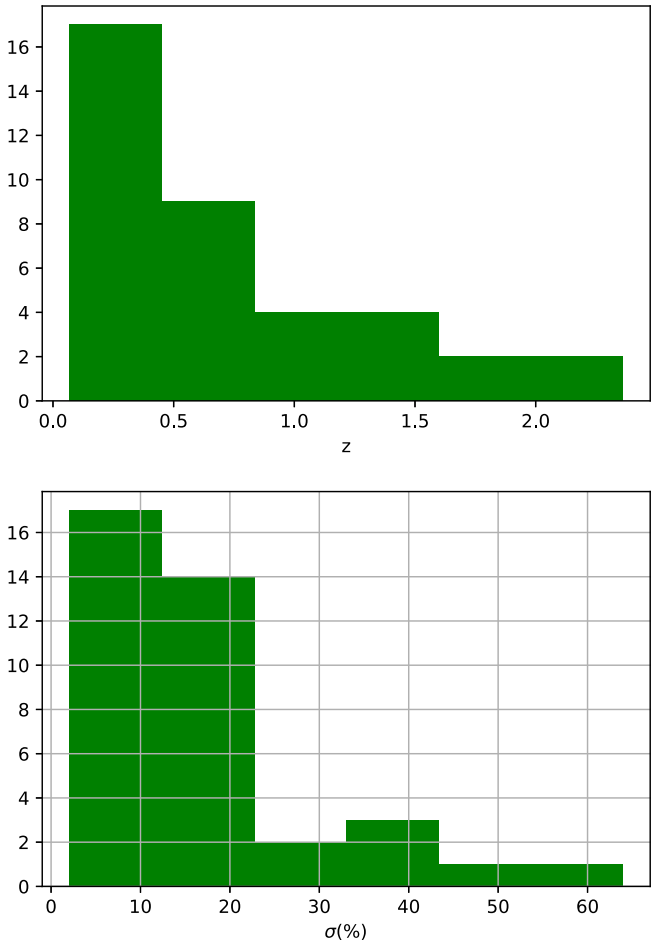

FIG. 1. The redshift (upper panel) and the relative error (lower panel) distributions of our data set.

components $\phi^{\mu+1}$ contain the free parameters which are related with the matter density, spatial curvature, and dark energy.

Therefore, in order to proceed with the statistical analysis, we need to either know the exact value of the Hubble constant or have it as a free parameter. The most recent results on the determination of the Hubble constant have found a $\sim 3.1\sigma$ tension between the value obtained by the SNIa project (Riess *et al.* [33]) of $H_0 = 73.24 \pm 1.74$ Km/s/Mpc and the results from Planck (see Ref. [1]) of $H_0 = 67.8 \pm 0.9$ Km/s/Mpc. The Hubble constant problem has inspired us to propose a technique which provides the chi-square estimator independent from the value of H_0. At this point, we present the basic ingredients toward marginalizing χ^2 over H_0.[2] Indeed, inserting (2) into (1), the latter equation simply becomes

$$\chi^2(\phi^\mu) = AH_0^2 - 2BH_0 + \Gamma, \tag{3}$$

where

$$A = \sum_{i=1}^{N} \frac{E^2(z_i)}{\sigma_i^2}$$

$$B = \sum_{i=1}^{N} \frac{E(z_i) H_D(z_i)}{\sigma_i^2}$$

$$\Gamma = \sum_{i=1}^{N} \frac{H_D(z_i)^2}{\sigma_i^2}.$$

In this context, the corresponding likelihood function is written as

$$\mathcal{L} = e^{-x^2/2} \Rightarrow \mathcal{L} = \exp\left[\frac{AH_0^2 - 2BH_0 + \Gamma}{2}\right] \tag{4}$$

or

$$\mathcal{L}(D|\phi^\mu, M) = \exp\left[\frac{A(H_0 - \frac{B}{A})^2 - \frac{B^2}{A} + \Gamma}{2}\right].$$

Using Bayes's theorem and marginalizing over H_0, we arrive at

$$p(\phi^\mu|D, M) = \frac{1}{p(D|M)} \int e^{-\frac{A(H_0 - B/A)^2 - B^2/A + \Gamma}{2}} dH_0. \tag{5}$$

Furthermore, considering that H_0 lies in the range $H_0 \in (0, +\infty)$, introducing the variable $y = H_0 - B/A$, and utilizing flat priors $p(\phi^\mu|M, H_0) = 1$, we obtain after some simple calculations

$$p(\phi^\mu|D, M) = \frac{1}{p(D|M)} e^{-\frac{1}{2}(\Gamma - B^2/A)} \int_{-\frac{B}{A}}^{+\infty} e^{-\frac{A}{2}y^2} dy \tag{6}$$

or

$$p(\phi^\mu|D, M) = \frac{1}{p(D|M)} e^{-\frac{1}{2}[\Gamma - \frac{B^2}{A}]} \sqrt{\frac{\pi}{2A}} \left[1 + \mathrm{erf}\left(\frac{B}{\sqrt{2A}}\right)\right], \tag{7}$$

where $\mathrm{erf}(x) = \frac{2}{\sqrt{\pi}} \int_0^x e^{-y^2} dy$ is the error function. Lastly, it is easy to show that the above likelihood function corresponds to the following marginalized $\tilde{\chi}_H^2$ function,

$$\tilde{\chi}_H^2(\phi^{\mu+1}) = \Gamma - \frac{B^2}{A} + \ln A - 2 \ln\left[1 + \mathrm{erf}\left(\frac{B}{\sqrt{2A}}\right)\right], \tag{8}$$

[2]Similar analysis has been proposed by Taddei and Amendola [43] and Basilakos and Nesseris [44]) in order to marginalize the chi-square function of the growth rate data over the value of the rms fluctuations at $8h^{-1}$ Mpc, namely σ_8.

where we have ignored the constant $\ln(\pi/2)$, since it does not play a role during the minimization procedure.

Obviously, the statistical estimator (8) does not suffer from the Hubble constant problem. Indeed, instead of minimizing χ^2, we now use the marginalized $\tilde{\chi}^2_H$ function which is independent of H_0, and thus we do not need to impose in the statistical analysis an *a priori* value for the Hubble constant, as is usually done in many other studies of this kind.

Bellow, we test the performance of the current statistical procedure at the expansion level using some well-known dark energy models.

III. FITTING MODELS TO $H(z)$ DATA

In this section, we present the expansion rate of the Universe in the context of the most basic DE models of which the free parameters are constrained following the procedure of the previous section. Due to the fact that the $H(z)$ data are well inside in the matter dominated era, we can neglect the radiation term from the Hubble expansion.

Let us now briefly discuss the cosmological models explored in the present study:

(i) In the nonflat ΛCDM model, the Hubble parameter is given by

$$E(z,\phi^{\mu+1}) = [\Omega_{m0}(1+z)^3 + \Omega_{\Lambda 0} + \Omega_{K0}(1+z)^2]^{1/2}, \tag{9}$$

where Ω_{K0} is the dimensionless curvature density parameter at the present time which is defined as $\Omega_{K0} = 1 - \Omega_{m0} - \Omega_{\Lambda 0}$; hence, the cosmological vector takes the form $\phi^{\mu+1} = (\Omega_{m0}, \Omega_{\Lambda 0})$.

(ii) In the wCDM spatially flat model, the equation-of-state parameter $w_d = p_d/\rho_d$ is constant [45], where ρ_d is the density and p_d is the pressure of the dark energy fluid respectively. Under the latter conditions, the normalized Hubble function is

$$E(z,\phi^{\mu+1}) = [\Omega_{m0}(1+z)^3 + \Omega_{d0}(1+z)^{3(1+w)}]^{1/2}, \tag{10}$$

where $\Omega_{d0} = 1 - \Omega_{m0}$ and thus the cosmological vector is $\phi^{\mu+1} = (\Omega_{m0}, w)$.

(iii) The Chevalier-Polarski-Linder (CPL) cosmological model was first introduced in the literature by Linder [46] and Chevalier and Polarski [47]. Here, the equation-of-state parameter is allowed to vary with redshift, and it is written as a first order Taylor expansion around the present epoch, $w(a) = w_0 + w_1(1-a)$ with $a = 1/(1+z)$. Therefore, the dimensionless Hubble parameter takes the following form,

$$E(z,\phi^{\mu+1}) = [\Omega_{m0}(1+z)^3 + \Omega_{d0}X(z)]^{1/2}, \tag{11}$$

where

$$X(z) = (1+z)^{3(1+w_0+w_1)} \exp\left(-3w_1\frac{z}{z+1}\right)$$

and $\Omega_{d0} = 1 - \Omega_{m0}$. In this case, the vector of the model parameters is $\phi^{\mu+1} = (\Omega_{m0}, w_0, w_1)$.

For the nonflat ΛCDM model, the likelihood function peaks at $(\Omega_{m0}, \Omega_{\Lambda 0}) = (0.250^{+0.039}_{-0.043}, 0.693^{+0.147}_{-0.186})$ with $\tilde{\chi}^2_{\rm H,min}/df \simeq 0.639$ (df are the degrees of freedom). Also, based on $\Omega_{K0} = 1 - \Omega_{m0} - \Omega_{\Lambda 0}$, we find $\Omega_{K0} = 0.057^{+0.142}_{-0.152}$. Our constraints are in agreement within 1σ errors with those of Farooq *et al.* [28], who found, using the same $H(z)$ data, $(\Omega_{m0}, \Omega_{\Lambda 0}) = (0.23, 0.60)$ for $H_0 = 68$ Km/s/Mpc and $(\Omega_{m0}, \Omega_{\Lambda 0}) = (0.25, 0.78)$ for $H_0 = 73.24$ Km/s/Mpc respectively. Recently, Jesus *et al.* [48] found $H_0 = 69.5 \pm 2.5$ Km/s/Mpc, $\Omega_{m0} = 0.242 \pm 0.036$ $\Omega_{\Lambda 0} = 0.256 \pm 0.14$, while using the Riess *et al.* [49] prior $H_0 = 73.8$ Km/s/Mpc, they found $0.21 \leq \Omega_{m0} \leq 0.32$ and $0.65 \leq \Omega_{\Lambda 0} \leq 0.99$.

In the case of wCDM cosmological model, the results of the minimization analysis are $(\Omega_{m0}, w) = (0.262^{+0.042}_{-0.037}, -0.96^{+0.275}_{-0.270})$ with $\tilde{\chi}^2_{\rm min}/df \simeq 0.64$. For comparison, Farooq *et al.* [28] obtained $(\Omega_{m0}, w_0) = (0.26, -0.86)$ for $H_0 = 68$ Km/s/Mpc and $(\Omega_{m0}, w_0) = (0.24, -1.06)$ for $H_0 = 73.24$ Km/s/Mpc respectively. Lastly, for the CPL parametrization, we find $\tilde{\chi}^2_{\rm min}/df \simeq 0.64$ and $(w_0, w_1) = (-0.960 \pm 0.171, 0.047 \pm 0.425)$, where we have set $\Omega_{m0} = 0.262$. We repeat our analysis by using the Ω_m-prior derived originally by the Planck team [1]. Specifically, if we impose $\Omega_{m0} = 0.308$, then we obtain $(w_0, w_1) = (-0.687 \pm 0.123, -1.009 \pm 0.598)$ with $\tilde{\chi}^2_{\rm H,min}/df \simeq 0.66$. Notice that in Table II we provide a more compact presentation of our statistical results. In Fig. 2, we plot the 1σ, 2σ, and 3σ confidence contours in the $(\Omega_{m0}, \Omega_{\Lambda 0})$ and (Ω_{m0}, w) planes for nonflat ΛCDM (upper panel) and wCDM (bottom panel) models respectively. We observe that our best-fit values are almost $\sim 1\sigma$ away from the values provided by the Planck team [1] (see the stars in Fig. 2). Moreover, in Fig. 3, we show the (w_0, w_1) contours for the CPL model by using $\Omega_{m0} = 0.262$ (upper panel) and $\Omega_{m0} = 0.308$ (bottom panel). The stars in Fig. 3 corresponds to the solution $(w_0, w_1) = (-1, 0)$. As expected, we find that the parameter w_0 is degenerate with respect to w_1, implying that the time varying equation-of-state parameter $w(z)$ is not constrained by this analysis.

A. Joint analysis with SNIa

Although the $H(z)$ data provide a direct measurement of the expansion of the Universe, due to their large errors with respect to the SNIa data, various authors preferred to utilize the latter data in order to constrain the cosmological parameters.[3] Here, we want to combine $H(z)$ and SNIa

[3]For a thorough treatment of the statistical difficulties, see Ref. [50].

TABLE II. Results of cosmological parameters values and uncertainties. Here, the $H(z)$ data are not correlated.

Models	Ω_{m0}	$\Omega_{\Lambda 0}(\Omega_{de})$	w_0	w_1	$\chi^2_{\rm min}/\nu$
		Using only the $H(z)$ data			
ΛCDM	$0.250^{+0.039}_{-0.043}$	$0.693^{+0.147}_{-0.186}$	-1	0	0.639
wCDM	$0.262^{+0.042}_{-0.037}$	0.738	$-0.960^{+0.275}_{-0.270}$	0	0.640
CPL	0.262	0.738	-0.960 ± 0.171	0.047 ± 0.425	0.640
CPL	0.308	0.692	-0.687 ± 0.123	-1.009 ± 0.598	0.657
		Using the joint analysis of $H(z)$/SNIa data			
ΛCDM	0.255 ± 0.020	0.692 ± 0.045	-1	0	0.950
wCDM	0.264 ± 0.015	0.736	-0.965 ± 0.046	0	0.950
CPL	0.264	0.736	-0.979 ± 0.260	0.085 ± 0.094	0.950
CPL	0.308	0.692	-0.938 ± 0.053	-0.684 ± 0.288	0.955

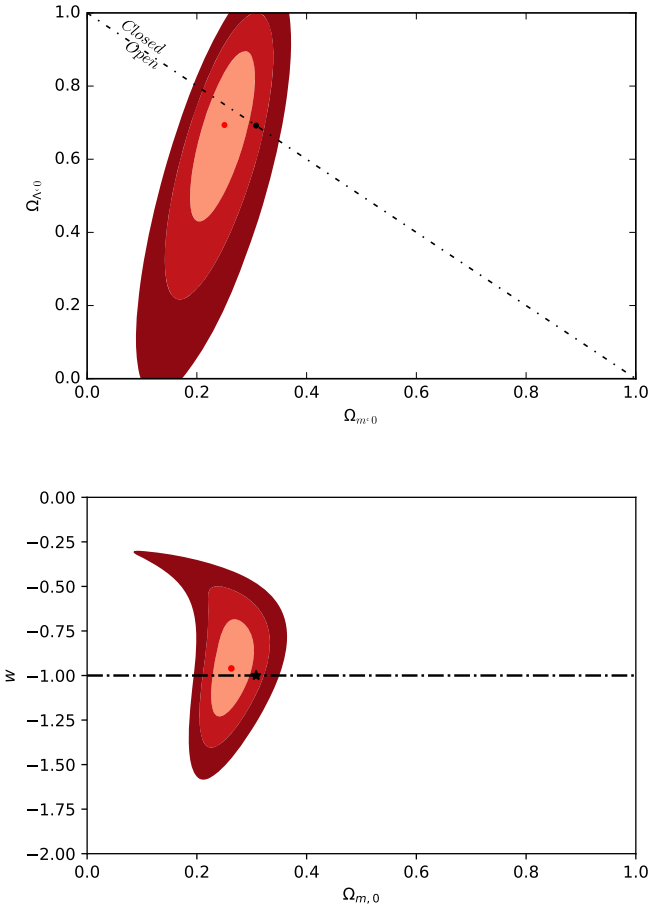

FIG. 2. The likelihood contours for $\Delta\tilde{\chi}^2 = \tilde{\chi}^2_H - \tilde{\chi}^2_{\rm H,min}$ equal to 1σ (2.32), 2σ (6.18), and 3σ (11.83) confidence levels. The red dot corresponds to the best-fit solutions. *Upper panel:* the contours of the nonflat ΛCDM model, in the $(\Omega_{m0}, \Omega_\Lambda)$ plane. The dashed line represents the $\Omega_{m0} + \Omega_\Lambda = 1$ line. Here, the best-fit point is $(\Omega_{m0}, \Omega_\Lambda) = (0.250, 0.693)$. *Lower panel:* the wCDM model in the (Ω_{m0}, w) plane. The best-fit solution is $(\Omega_{m0}, w) = (0.262, -0.960)$. The dashed curve corresponds to $w = -1$. Notice that stars show the best-fit solution provided by the Planck team [1] for the flat ΛCDM model.

in order to study the performance of the $H(z)$ data (as they stand today, namely 38 entries) with that of SNIa data. In particular, we use the *Union 2.1* set of 580 SNIa of Suzuki *et al.* [5]. Concerning the chi-square estimator of the SNIa, we utilize the method of Ref. [51], where the form of $\tilde{\chi}^2_{\rm Sn}$ is independent of H_0 (see also Ref. [9] and references

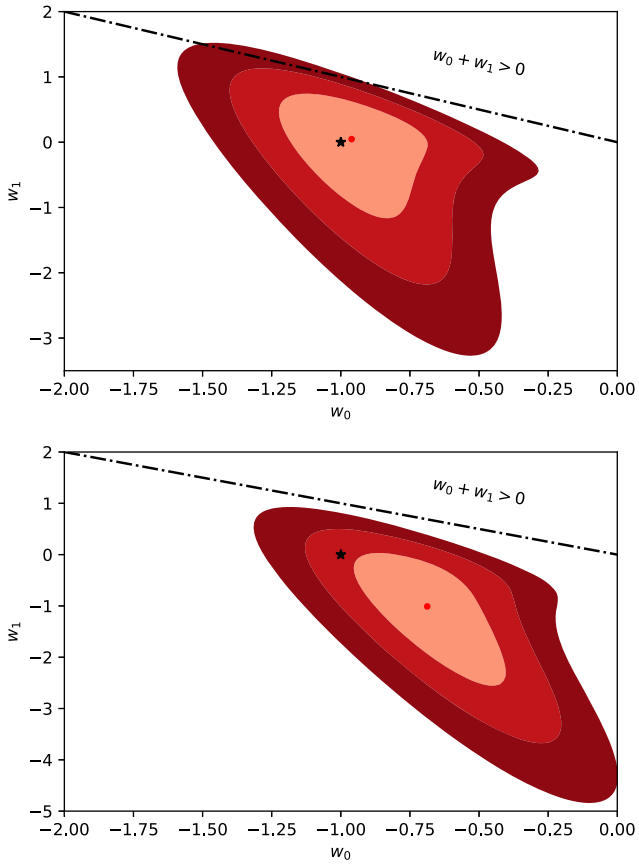

FIG. 3. The likelihood contours $\Delta\tilde{\chi}^2 = \tilde{\chi}^2_H - \tilde{\chi}^2_{\rm H,min}$ in the case of CPL model. *Upper panel:* Here, we utilize $\Omega_{m0} = 0.262$ from the first panel of Table II. *Bottom panel:* Here, we use $\Omega_{m0} = 0.308$ from Planck, [1]. Notice that stars corresponds to flat ΛCDM model $(w_0, w_1) = (-1, 0)$.

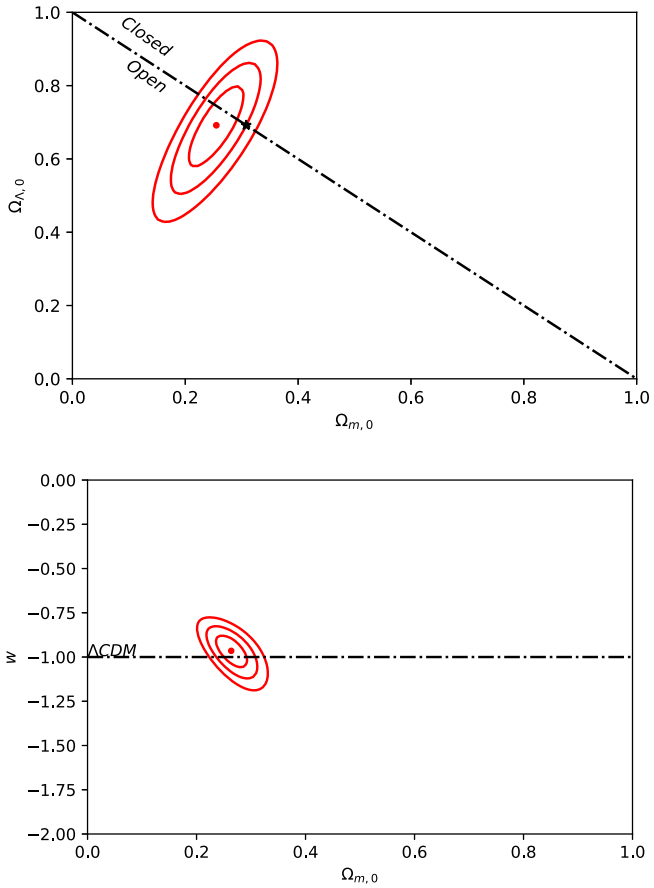

FIG. 4. The $H(z)$/SNIa joint likelihood contours. The upper panel shows the solution space for the nonflat ΛCDM model, while the lower panel corresponds to the wCDM model. The dashed line corresponds to $w = -1$. The red dot corresponds to the best-fit solutions. The black star shows the solution of Planck [1].

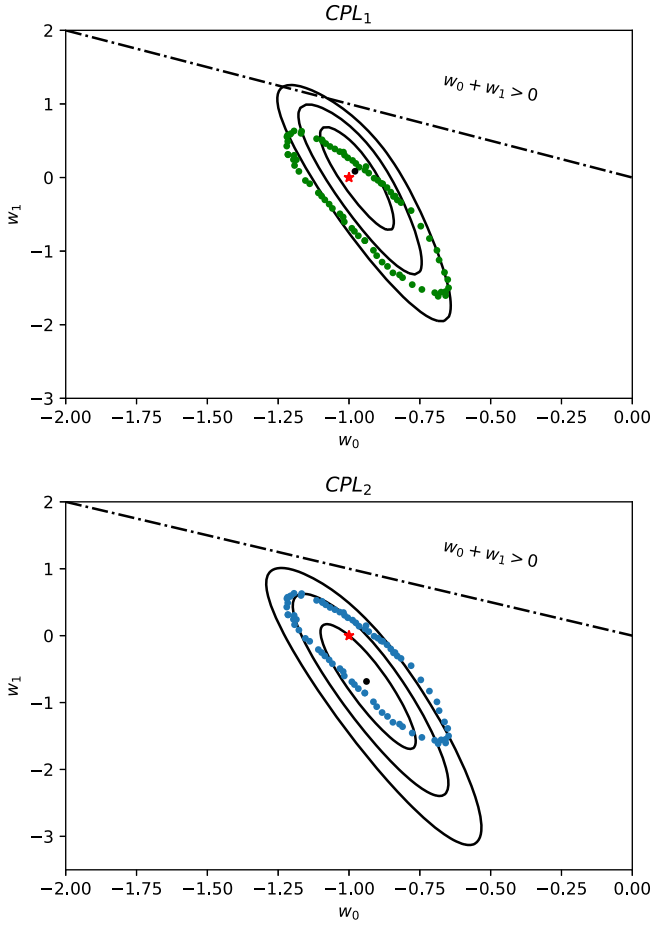

FIG. 5. The joint SNIa and $H(z)$ likelihood contours in the (w_0, w_1) plane for $\Omega_{m0} = 0.262$ (upper panel) and $\Omega_{m0} = 0.308$ (lower panel). The solid black dots correspond to the best-fit parameters. We also show the theoretical ΛCDM $(w_0, w_1) = (-1, 0)$ values (star points). The dot-dashed line corresponds to $w_0 + w_1 = 0$. Finally, the area of green/blue dots is borrowed from Planck [1].

therein). In this framework, the overall likelihood function is given by the product of the individual likelihoods according to

$$\mathcal{L}_{\rm tot} = \mathcal{L}_{\rm sn} \times \mathcal{L}_H,$$

which translates in an addition for the total $\chi^2_{\rm tot}$:

$$\chi^2_{\rm tot} = \tilde{\chi}^2_{\rm sn} + \tilde{\chi}^2_H.$$

The results based on the joint analysis of $H(z)$/SNIa data are given in Figs. 4 and 5 and listed in the second panel of Table II. It becomes clear that the addition of the SNIa data in the likelihood analysis improves substantially the statistical results. Overall, we find that the $H(z)$/SNIa joint analysis increases the figure of merit (FoM; for a definition, see below) by a factor of ∼2.5 with respect to that of $H(z)$ analysis. Therefore, the combined analysis of the $H(z)$ data with SNIa reduces significantly the parameter space, providing tight constraints on the nonflat ΛCDM and wCDM models respectively. In particular, for the former model, the total likelihood function peaks at $(\Omega_{m0}, \Omega_{\Lambda 0}) = (0.255 \pm 0.02, 0.692 \pm 0.045)$ with $\chi^2_{\rm tot,min}/df \simeq 0.950$, while for the latter cosmological model, we find $(\Omega_{m0}, w) = (0.264 \pm 0.015, -0.965 \pm 0.046)$ with $\chi^2_{\rm tot,min}/df \simeq 0.950$. Concerning the CPL model, we find that, although the area of $w_0 - w_1$ contours is significantly reduced, the degeneracy between w_0 and w_1 persists also in the joint analysis. However, what is specifically interesting is that for the CPL model the $H(z)$/SNIa contours are in very good agreement with those of Planck TT, lowP CMB data and external (BAO, JLA, and H_0) data [1] (see the solid circles in Fig. 5), which confirms that our analysis with the $H(z)$ and SNIa probes correctly reveals the expansion history of the Universe as provided by the Planck team.

Concluding this section, it is interesting to mention that recently Yu *et al.* [52] introduced the covariance matrix of three BAO $H(z)$ measurements [11] in the $H(z)$ analysis.

TABLE III. Cosmological constraints using the correlation matrix of the $H(z)$ data [11,52].

Models	Ω_{m0}	$\Omega_{\Lambda 0}(\Omega_{de})$	w_0	w_1	$\chi^2_{\rm min}/\nu$
		Using only the $H(z)$ data			
ΛCDM	0.255 ± 0.026	0.692 ± 0.142	-1	0	0.747
wCDM	0.248 ± 0.024	0.752	-1.015 ± 0.177	0	0.750
CPL	0.248	0.752	-1.011 ± 0.332	-0.110 ± 0.122	0.749
CPL	0.308	0.692	-0.565 ± 0.221	-1.564 ± 0.731	0.738
		Using the joint analysis of $H(z)$/SNIa data			
ΛCDM	0.248 ± 0.016	0.701 ± 0.065	-1	0	0.958
wCDM	0.257 ± 0.005	0.743	-0.954 ± 0.005	0	0.957
CPL	0.257	0.748	-0.946 ± 0.096	-0.106 ± 0.362	0.957
CPL	0.308	0.692	-0.761 ± 0.114	-1.052 ± 0.551	0.969

Using this covariance matrix, we have redone our statistical analysis, and in Table III, we provide the corresponding constraints, which are in agreement (within 1σ errors) with those of Table II. Notice that in the Appendix we have generalized the statistical methodology of Sec. II in the presence of the covariance matrix.

IV. STRATEGY TO IMPROVE THE COSMOLOGICAL CONSTRAINS USING THE $H(z)$ DATA

From the previous analysis, it becomes clear that an important question that we need to address is the following: What is the strategy for the recovery of the dark energy equation of state using the direct measurements of the Hubble expansion? In this section, we proceed with our investigation toward studying the effectiveness of utilizing $H(z)$ measurements to constrain the equation-of-state parameter. Specifically, our aim is to test how much better can we go in placing cosmological constraints by increasing the current $H(z)$ sample from 38 to 100. In order to achieve such a goal, we produce sets of Monte Carlo simulations with which we quantify our ability to recover the input cosmological parameters of a fiducial cosmological model, namely $(\Omega_{m0}, \Omega_{K0}, w_0, w_1) = (0.25, 0, -1, 0)$ with $H_0 = 68.75$ Km/s/Mpc. In the upper panel of Fig. 6, we present the evolution of the Hubble parameter of the reference model (black line), and on top of that, we plot the $H(z)$ data (solid points). In the lower panel of Fig. 6, we show the distribution of $100(\%) \times |H_D - H_{\rm ref}|/H_D$ as a function of redshift (see below), where H_D and $H_{\rm ref}$ are the Hubble parameters of the data and the reference cosmology respectively. We verify that the differences $\delta H = |H_D - H_{\rm ref}|$ are not correlated with redshift.

Now, we develop an algorithm that generates different numbers of mock $H_{\rm MC}(z)$ measurements following the redshift and the error distributions of the real $H(z)$ data (see Figs. 1 and 2). Thus, our aim is to obtain the value of $H_{\rm MC}$ as well as the corresponding 1σ error by calibrating the mock $H(z)$ sample from the real $H(z)$ data in which $0.07 \leq z \leq 2.36$. More specifically, we implement the following steps.

First, from the redshift interval [0.07, 2.36], we choose a redshift $z_{\rm ran}$ by randomly sampling the observed redshift

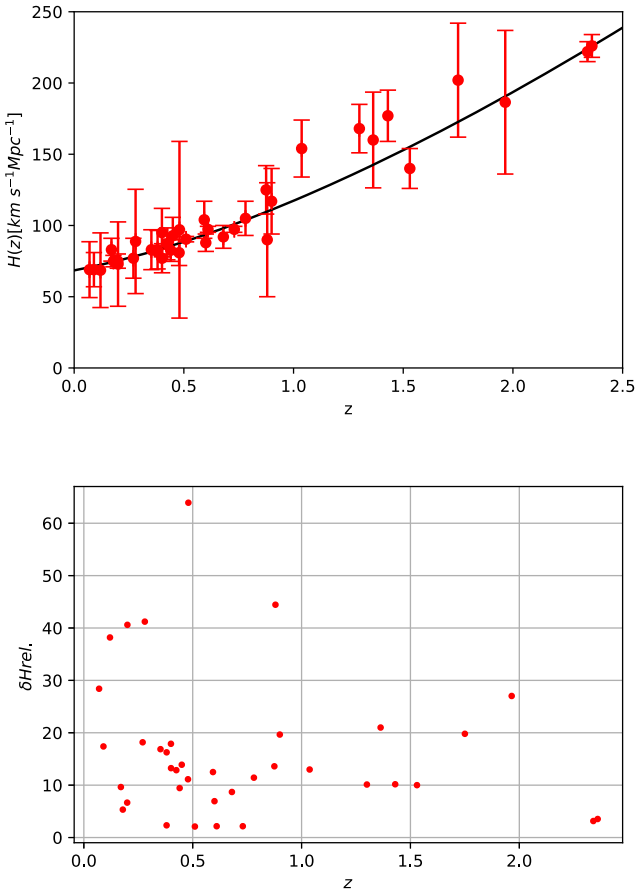

FIG. 6. *Upper panel:* Comparison of the observed (red points [28]) and theoretical evolution of the reference Hubble parameter, $H(z)$, using $(\Omega_{m0},\Omega_{K0},w_0,w_1)=(0.25,0,-1,0)$ and $H_0 = 68.75$ Km/s/Mpc. The reference cosmology is represented by the solid curve. *Lower panel:* The distribution of $\delta H = |H_D - H_{\rm ref}|$. Notice that $H_D(z)$ indicates the observed Hubble parameter, while $H_{\rm ref}(z)$ is the Hubble function of the fiducial cosmology.

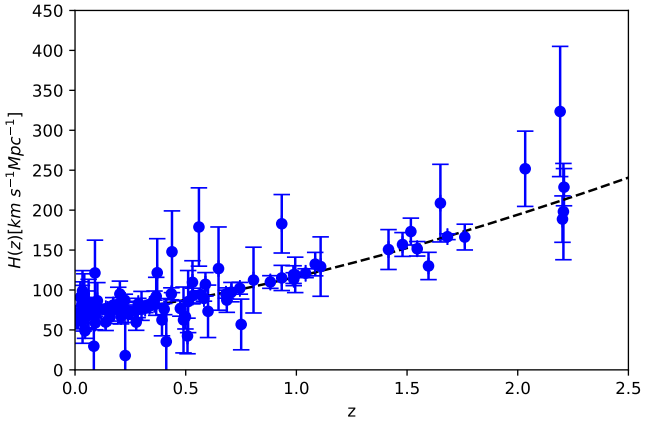

FIG. 7. The mock Hubble parameter as a function of redshift. In this case, the mock data set constraints $N = 100$ entries. The dashed line corresponds to the ΛCDM model with $(H_0, \Omega_{m0}, \Omega_{\Lambda 0}) = (68.5, 0.25, 0.693)$.

distribution (see Fig. 1). For this "random" redshift, we define the measured Hubble parameter $H_D(z_{\rm ran})$ and the ideal Hubble parameter $H_{\rm ref}(z_{\rm ran})$ from the reference cosmology. Second, in order to take into account the deviation of the observed Hubble parameter from the reference cosmology, we are randomly sampling the distribution of the differences δH (see the lower panel of Fig. 6) between the data and the fiducial cosmological model. Once first and second steps are completed for all mock data[4] used, the mock Hubble parameter $H_{\rm MC}$ is selected from the normal distribution $\mathcal{N}(H_{\rm ref}, \sigma^2_{\rm ran})$. Finally, performing a trial and error procedure, we have confirmed that by assigning to each mock Hubble parameter $H_{\rm MC}$ the individual error $\sigma_{\rm ran} = \sqrt{\sigma_H^2 + \delta H^2}$ we recover the contours of the reference model, and thus the mock $H(z)$ data contain the simulated triads $\{z_{\rm ran}, H_{\rm MC}, \sigma_{\rm ran}\}_i$, where $i = 1, ..N$ and $N \in [38, 120]$. For the benefit of the reader in Fig. 7, we plot the mock Hubble parameter as a function of redshift. Notice that in this case the mock sample contains $N = 100$ entries. This figure can be compared with that of the observed $H(z)$ data (see the upper panel of Fig. 6).

Now, based on the mock data, we attempt to measure the effectiveness of the $H(z)$ measurements in constraining the cosmological parameters. Therefore, we calculate the well-known FoM in the solution space. The figure-of-merit (FoM) is a useful tool because it provides an assess how constraining the likelihood analysis of the $H(z)$ data can be. We have defined the FoM as the inverse of the enclosed area of the 2σ contour in the parameter space of any two degenerate cosmological parameters, namely $\Omega_{m0} - \Omega_{\Lambda 0}$ and $w_0 - w_1$. Of course, the higher the FoM is, the more constraining the model is. We generate 100 Monte Carlo

[4]We sample the number of mock data as $N \in [38, 120]$ in steps of 2.

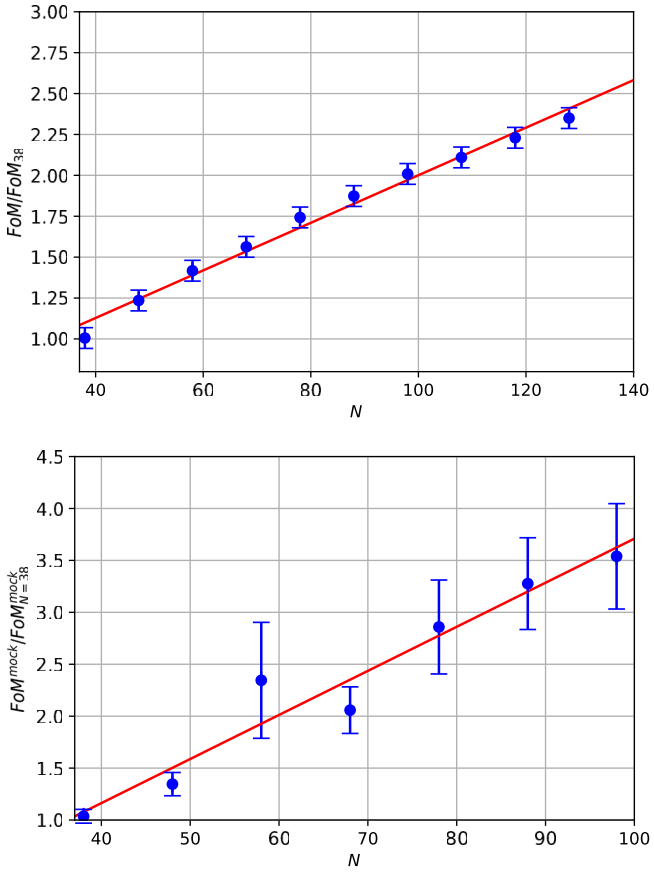

FIG. 8. The FoM/FoM_{38} as a function of the number of entries in the mock $H(z)$ data. Notice, that we used 100 realizations. The quantity FoM_{38} is the figure of merit of the current $H(z)$ data. The upper and lower panels correspond to nonflat ΛCDM and CPL models respectively.

simulations for each selected number $(N = 38, 40, ..120)$ of mock $H(z)$ data, and the corresponding results are shown in Fig. 8. In this figure, we plot the ratio between the simulation FoM and that of the present sample of 38 $H(z)$ measurements, namely $\rm FoM_{38}$, as a function of the number of mock $H(z)$ data. Therefore, with the aid of Fig. 8, we see the behavior of the factor by which the FoM increases with respect to its present value. We observe that this factor increases linearly with the number of $H(z)$ mock data. A linear regression yields

$$\left(\frac{FoM}{FoM_{38}}\right)_{\text{non-flat},\Lambda} = (0.0087 \pm 0.0002)N + 0.689 \pm 0.027$$

$$\left(\frac{FoM}{FoM_{38}}\right)_{\rm CPL} = (0.0246 \pm 0.0007)N - 0.534 \pm 0.33.$$

Using the above expressions, we find that for the realistic future observations of ∼100 $H(z)$ data the FoM is expected to increase by factors of ∼2 and ∼3 for the nonflat ΛCDM and CPL models respectively.

V. DISCUSSION

In this section, we provide a qualitative discussion of our $H(z)$ based analysis, giving the reader the opportunity to appreciate the new results of our study. First of all, to our knowledge, this is the first time that a Bayesian likelihood analysis applied on the $H(z)$ data, marginalizing properly the value of H_0 and thus excluding it from the likelihood analysis. But why is this important in these kind of studies? Using the direct measurements of the cosmic expansion, namely $H(z)$ data in constraining the cosmological models, via the standard χ^2 estimator [see Eq. (1)], one has to either know the exact value of the Hubble constant or have it as a free parameter, increasing, however, the parameter space. If we follow the first path, then we are facing the well-known Hubble constant problem. This problem is related with the fact that the determination of the Hubble constant has indicated a $\sim 3.1\sigma$ tension between the value obtained by the Planck team (see Ref. [1]), namely $H_0 = 67.8 \pm 0.9$ Km/s/Mpc and the results provided by the SNIa project (Riess *et al.* [33]) of $H_0 = 73.24 \pm 1.74$Km/s/Mpc. This is the main reason that various studies in the literature first imposed the Hubble constant to the above values and then they placed constraints to other cosmological parameters $(\Omega_m, \Omega_\Lambda, w, ..)$. For example, Farooq *et al.* [28] provided two different sets of constraints for different values of H_0. Indeed, if they imposed $H_0 = 68$ Km/s/Mpc, then their likelihood function peaks at $(\Omega_{m0}, \Omega_{\Lambda 0}) = (0.23, 0.60)$, while for $H_0 = 73.24$ Km/s/Mpc, the corresponding likelihood function peaks at a different pair, namely $(\Omega_{m0}, \Omega_{\Lambda 0}) = (0.25, 0.78)$. Obviously, the fact that the exact value of the Hubble constant remains an open issue in cosmology affects the constraints. At this point, we would like to stress that our statistical method (see Sec. II) treats in a natural way the aforementioned problem. Specifically, the outcome of our analysis is a new chi-square estimator [see Eq. (8)] which is not affected by the value of the Hubble constant, and thus our constraints are independent from H_0.

Concerning the importance of having direct measurements of the cosmic expansion, some considerations are in order at this point. The choice of $H(z)$ data, used in many studies in the literature as well as in our work, is dictated by the fact that these data are the only data which are giving a direct measurement of the Hubble expansion as a function of redshift. To date, the cosmic acceleration has been traced mainly by SNIa, which means that the observed Hubble relation, namely distance modulus versus z, lies in the range $0 < z < 1.5$ [5,6]. In general, the cosmological data used to probe the cosmic expansion history involve a combination of standard candles (SNIa, GRBs, HII), standard rulers (clusters, BAOs, CMB shift parameters) and the CMB angular power spectrum. These observations probe the integral of the Hubble expansion rate $H(z)$; hence, they give us indirect information of the cosmic expansion either up to redshifts of order $z \simeq 1$–1.5 (SNIa, BAO, and clusters) or up to the redshift of recombination ($z \sim 1100$). It is therefore clear that the redshift range $\sim$1.5–1000 is not directly probed by any of the aforementioned observations, and as shown in Ref. [8], the redshift range $1.5 < z < 3.5$ plays a vital role in constraining the DE equation of state, since different DE models reveal their largest differences in this redshift interval. Therefore, the fact that direct $H(z)$ measurements can be extracted relatively easily at high redshifts make them, especially those which are visible at redshifts $z > 1.5$, indispensable tools for investigating the phenomenon of the accelerated expansion of the Universe. It is worth mentioning that there are proposed methods which potentially could expand the $H(z)$ measurements to $z \leq 5$ [32] (for other possible tracers, see Refs. [7,9]).

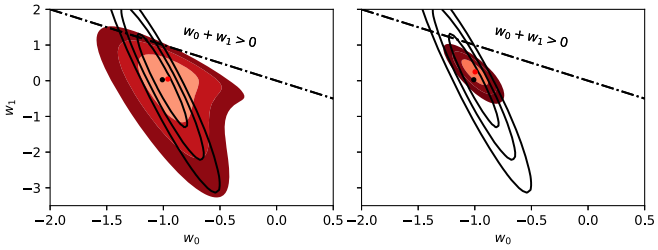

FIG. 9. *Left panel:* The 1σ, 2σ, and 3σ likelihood contours in the case of the current $H(z)$ sample, using the CPL parametrization. *Right panel:* The corresponding contours in the case of our mock sample which contains $\sim$100 entries. In black, we show the SNIa contours of the *Union 2.1* set.

At the moment, an obvious disadvantage of using the current $H(z)$ sample alone in constraining the dark energy models is related with the small number statistics and thus with the weak statistical constraints. However, in order to appreciate the impact of the current $H(z)$ data set in constraining the dark energy models, we show in Sec. II A that our combined $H(z)$/SNIa statistical analysis (which is not affected by H_0) correctly reveals the expansion of the Universe as provided by the team of Planck [1]. Specifically, we find that for the CPL model the $H(z)$/SNIa the $w_0 - w_1$ solution space is compatible with that of Planck TT, lowP CMB data and external (BAOs, JLA, H_0) data; see the solid circles in Fig. 5). In order to understand the effectiveness of the $H(z)$/SNIa test in constraining the $w_0 - w_1$ parameter space, we present in the left panel of Fig. 9 the $H(z)$ (red-scale contours) and *Union 2.1* SNIa (solid black curves) contours respectively. We observe that, even with the current $H(z)$ contours, the joint $H(z)$/SNIa analysis reduces significantly (due to different inclination of the contours) the $w_0 - w_1$ solution space and hence it becomes compatible to that of the Planck (TT, lowP CMB, BAOs, JLA, and H_0) test.

Therefore, from the above discussion, it becomes clear that the ideal avenue that cosmologists need to follow toward understanding the nature of the cosmic acceleration is to use future high quality $H(z)$ data to measure the dark energy equation of state and the matter content of the Universe. This issue is discussed in Sec. IV. In particular, Monte Carlo predictions show that for the realistic future expectations of $\sim$100 $H(z)$ measurements we predict that the present FoM of the nonflat ΛCDM model is increased

by a factor of 2, while in the case of the CPL parametrization we find a threefold increase of the corresponding FoM. For an example, we provide in the right panel of Fig. 9 the contours of one simulation of 100 $H(z)$ measurements for the CPL model in the $w_0 - w_1$ plane (red-scale contours) For comparison, we plot the corresponding contours (black curves) of the *Union 2.1* set of 580 SNIa of Suzuki *et al.* [5]. Obviously, in the case of SNIa data, we observe that the parameters w_0 and w_1 are degenerate. This seems to hold also for the JLA data [6]. However, our Monte Carlo analysis indicates that with the aid of only $\sim$100 future $H(z)$ measurements in the redshift range $0 < z < 2.4$, we will be able to put strong constraints on w_0 as well as to reduce significantly the w_1 uncertainty. The latter is important since the w_1 parameter tests the evolution of the DE equation-of-state parameter. We argue that, having the future $H(z)$ data available, we will be in a position to use these data combined with SNIa and other probes to whittle away the available parameter space for the contender dark matter/energy scenarios and hopefully to settle on a single viable model.

In a nutshell, we would like to make clear that with the present analysis we do not want to compete with SNIa or other cosmological probes. The aim of our article is to investigate the power of direct measurements of the cosmic expansion, toward constraining the dark energy models, and to provide the appropriate observational framework for future work.

VI. CONCLUSIONS

We investigated the performance of the latest expansion data, the so-called $H(z)$ measurements, toward constraining the dark energy models. In the context of $H(z)$ data aimed at testing the various forms of dark energy, it is important to minimize the amount of priors needed to successfully complete such a task. One such prior is the Hubble constant, and its measurement at the $\sim$1% accuracy level has been proposed as a necessary step for constraining the dark energy models. However, it is well known that the best choice of the value of H_0 is rather uncertain; namely, a $\sim 3.1\sigma$ tension has been found between the value provided by the Planck team (see Ref. [1]) and the results obtained by the SNIa project (Riess *et al.* [33]). In order to circumvent this problem, we implemented in the first part of our work a statistical method which is not affected by the value of H_0. Based on the latter approach, we found that the $H(z)$ data do not rule out the possibility of either nonflat models or dynamical dark energy cosmological models.

Then, we performed a joint likelihood analysis using the $H(z)$ and the SNIa data, thereby putting tight constraints on the cosmological parameters, namely $\Omega_{m0} - \Omega_{\Lambda 0}$ (nonflat ΛCDM model) and $\Omega_{m0} - w$ (wCDM model). Furthermore, using the CPL parametrization, we found that the $w_0 - w_1$ parameter space provided by the $H(z)$/SNIa joint analysis is in a very good agreement with that of Planck 2015, which confirms that the present analysis with the $H(z)$ and SNIa probes correctly captures the expansion of the Universe as found by the team of Planck.

Finally, we performed sets of Monte Carlo simulations in order to quantify the ability of the $H(z)$ data to provide strong constraints on the model parameters. The Monte Carlo approach showed substantial improvement of the constraints, when increasing the sample to $\sim$100 $H(z)$ measurements. Such a target can be achieved in the future, especially in the light of the next generation of surveys.

ACKNOWLEDGMENTS

S. Basilakos acknowledges support by the Research Center for Astronomy of the Academy of Athens in the context of the program "Testing general relativity on cosmological scales" (Reference No. 200/872).

APPENDIX: INCLUDING COVARIANCE IN THE STATISTICAL ANALYSIS

With the aid of the our statistical method (see Sec. II), we calculate the new chi-square estimator that is relevant in the case of the covariance matrix. If the data are correlated, then the chi-square estimator is written as

$$\chi^2_H = \mathbf{V}\mathbf{C}^{-1}_{\rm cov}\mathbf{V}^T, \tag{A1}$$

where $\mathbf{C}^{-1}_{\rm cov}$ is the inverse of the covariance matrix [52] and

$$\mathbf{V} = \{H_{\rm obs}(z_1) - H_M(z_1, \phi^\mu), \ldots, H_{\rm obs}(z_N) - H_M(z_N, \phi^\mu)\},$$

or using Eq. (2), we have

$$\mathbf{V} = \{H_{\rm obs}(z_1) - H_0 E(z_1, \phi^{\mu+1}), \ldots, H_{\rm obs}(z_N) - H_0 E(z_N, \phi^{\mu+1})\}.$$

Inserting the latter vector into Eq. (A1), we obtain after some algebra

$$\chi^2_H = A H_0^2 - 2BH_0 + \Gamma,$$

and thus following the procedure of Sec. II, the functional form of the marginalized $\tilde{\chi}^2_H$ estimator boils down to that of Eq. (8). Notice that the quantities A, B, and Γ are given by

$$A = \mathbf{E}\mathbf{C}^{-1}_{\rm cov}\mathbf{E}^T,$$

$$B = \frac{1}{2}(\mathbf{E}\mathbf{C}^{-1}_{\rm cov}\mathbf{H}^T_{\rm obs} + \mathbf{H}_{\rm obs}\mathbf{C}^{-1}_{\rm cov}\mathbf{E}^T),$$

$$\Gamma = \mathbf{H}_{\rm obs}\mathbf{C}^{-1}_{\rm obs}\mathbf{H}^T_{\rm obs},$$

with

$$\mathbf{E} = \{E(z_1, \phi^{\mu+1}), \ldots, E(z_N, \phi^{\mu+1})\}$$

and

$$\mathbf{H}_{\rm obs} = \{H_{\rm obs}(z_1), .., H_{\rm obs}(z_N)\}.$$

[1] Planck Collaboration, Astron. Astrophys. **594**, A13 (2016).
[2] L. Amendola and S. Tsujikawa, *Dark Energy: Theory and Observations Hardcover* (Cambridge University Press, Cambridge, England, 2010).
[3] R. Durrer and R. Maartens, *Dark Energy: Observational & Theoretical Approaches*, edited by P. Ruiz-Lapuente (Cambridge University Press, Cambridge, UK, 2010), p. 48.
[4] A. G. Kim *et al.*, Astropart. Phys., **63**, 2 (2015).
[5] N. Suzuki *et al.*, Astrophys. J. **746**, 85 (2012).
[6] M. Betoule *et al.*, Astron. Astrophys. **A22**, 568 (2014).
[7] L. Amati *et al.*, Astrophys. J. **390**, 81 (2002); G. Ghirlanda, G. Ghisellini, and C. Firmani New J. Phys., **8**, 123 (2006); S. Basilakos and L. Perivolaropoulos, Mon. Not. R. Astron. Soc. **391**, 411 (2008); F. Y. Wang, Z. G. Dai, and E. W. Liang, New Astron. Rev. **67**, 1 (2015).
[8] M. Plionis, R. Terlevich, S. Basilakos, F. Bresolin, E. Terlevich, J. Melnick, and R. Chavez, Mon. Not. R. Astron. Soc. **416**, 2981 (2011).
[9] R. Chavez, M. Plionis, S. Basilakos, R. Terlevich, E. Terlevich, J. Melnick, F. Bresolin, and A. L. González-Morán, Mon. Not. R. Astron. Soc., **462**, 2431 (2016).
[10] C. Blake *et al.*, Mon. Not. R. Astron. Soc. **418**, 1707 (2011).
[11] S. Alam *et al.*, Mon. Not. R. Astron. Soc. **470**, 2617 (2017).
[12] E. Calabrese, N. Battaglia, and D. N. Spergel, Classical Quantum Gravity **33**, 165004 (2016).
[13] S. Nesseris, G. Pantazis, and L. Perivolaropoulos, Phys. Rev. D **96**, 023542 (2017); S. Basilakos and S. Nesseris, Phys. Rev. D **96**, 063517 (2017).
[14] Y. Wang and M. Tegmark, Phys. Rev. D **71**, 103513 (2005).
[15] C. Shapiro and M. S. Turner, Astrophys. J. **649**, 563 (2006).
[16] L. Samushia and B. Ratra, Astrophys. J. Lett. **650**, L5 (2006).
[17] O. Farooq and B. Ratra, Astrophys. J. Lett. **766**, L7 (2013).
[18] L. P. Chimento, M. G. Richarte, and I. E. S. Garcia, Phys. Rev. D **88**, 087301 (2013).
[19] P. C. Ferreira, D. Pavón, and J. C. Carvalho, Phys. Rev. D **88**, 083503 (2013).
[20] S. Capozziello, O. Farooq, O. Luongo, and B. Ratra, Phys. Rev. D **90**, 044016 (2014).
[21] C. Gruber and O. Luongo, Phys. Rev. D **89**, 103506 (2014).
[22] M. Forte, Gen. Relativ. Gravit. **46**, 1811 (2014).
[23] T. Dankiewicz, M. P. Dabrowski, C. J. A. P. Martins, and P. E. Vielzeuf, Phys. Rev. D **89**, 083514 (2014).
[24] R.-G. Cai, Z.-K. Guo, and T. Yang, Phys. Rev. D **93**, 043517 (2016).
[25] F. Melia and T. M. McClintock, Astron. J. **150**, 119 (2015).
[26] Y. Chen, S. Kumar, and B. Ratra, Astrophys. J. **835**, 86 (2017).
[27] A. Mukherjee and N. Banerjee, Phys. Rev. D **93**, 043002 (2016).
[28] O. Farooq, F. R. Madiyar, S. Crandall, and B. Ratra, Astrophys. J. **835**, 26 (2017).
[29] R. C. Nunes, S. Pan, and E. Saridakis, J. Cosmol. Astropart. Phys. 08 (2016) 11.
[30] J. Magana *et al.*, arXiv:1706.09848v1.
[31] R. F. Nunes, S. Pan, E. N. Saridakis, and E. M. C. Abreu, J. Cosmol. Astropart. Phys. 01 (2017) 005.
[32] C. Pier-Stefano, D. Huterer, and A. Melchiorri, Phys. Rev. **75**, 062001 (2007).
[33] A. G. Riess *et al.*, Astrophys. J., **826**, 56 (2016).
[34] C. Zhang *et al.*, Res. Astron. Astrophys. **14**, 1215 (2014).
[35] J. Simon, L. Verde, and R. Jimenez, Phys. Rev. D **71**, 123001 (2005).
[36] M. Moresco *et al.*, J. Cosmol. Astropart. Phys. 08 (2012) 006.
[37] M. Moresco *et al.*, J. Cosmol. Astropart. Phys. 05 (2016) 014.
[38] C. Blake *et al.*, Mon. Not. R. Astron. Soc. **425**, 405 (2012).
[39] D. Stern, R. Jimenez, L. Verde, S. Adam Stanford, and M. Kamionkowski, Astrophys. J. Suppl. Ser. **188**, 280 (2010).
[40] M. Moresco Mon. Not. R. Astron. Soc. Lett. **450**, L16 (2015).
[41] T. Delubac *et al.*, Astron. Astrophys. **574** (2015) A59.
[42] A. Font-Ribera *et al.*, J. Cosmol. Astropart. Phys. 05 (2014) 027.
[43] L. Taddei and L. Amendola, J. Cosmol. Astropart. Phys. 02 (2015) 001.
[44] S. Basilakos and S. Nesseris, Phys. Rev. D **94**, 123525 (2016).
[45] M. S. Turner and M. White, Phys. Rev. D **56**, R4439 (1997); T. Chiba, N. Sugiyama, and T. Nakamura, Mon. Not. R. Astron. Soc. **289**, L5 (1997); J. A. S. Lima and J. S. Alcaniz, Astron. Astrophys. **357**, 393 (2000); Astrophys. J. **566**, 15 (2002).
[46] E. V. Linder, Phys. Rev. Lett. **90**, 091301 (2003).
[47] M. Chevallier and D. Polarski, Int. J. Mod. Phys. D **10**, 213 (2001).
[48] J. F. Jesus, T. M. Gregorio, F. Adrade-Oliveira, R. Valentim, and C. A. O. Matos, arXiv:1709.00646.
[49] A. G. Riess, L. Macri, S. Casertano, H. Lampeitl, H. C. Ferguson, A. V. Filippenko, S. W. Jha, W. Li, and R. Chornock, Astrophys. J. **730**, 119 (2011); **732**, 129(E) (2011).
[50] D. Rubin *et al.*, Astrophys. J. **813**, 137 (2015).
[51] S. Nesseris and L. Perivolaropoulos, Phys. Rev. D **72**, 123519 (2005).
[52] H. Yu, B. Ratra, and F.-Y. Wang, arXiv:1711.0343.